

Potential Energy Surfaces for Mo + CO and W + CO

Hang Tan,^{†,‡} Muzhen Liao,[‡] Dingguo Dai,[†] and K. Balasubramanian^{†,*}

Department of Chemistry and Biochemistry, Arizona State University, Tempe, Arizona 85287-1604,
Center for Advanced Study and Department of Chemistry, Tsinghua University, Beijing, 100084, China

Received: December 29, 1997; In Final Form: May 6, 1998

Potential energy surfaces for MoCO and WCO have been studied using the complete active space multiconfiguration self-consistent field (CAS-MCSCF) followed by multireference singles + doubles configuration interaction (MRSDCI). Spin-orbit effects are included through the relativistic configuration interaction (RCI) method for W-CO. Although at the CASSCF level the lowest ${}^7\Sigma^+$ state does not form a very stable minimum for WCO relative to $W({}^7S) + CO({}^1\Sigma^+)$, at the higher MRSDCI level not only does this state form a minimum but the ${}^5\Phi$ and ${}^5\Sigma^+$ states become nearly-degenerate with ${}^7\Sigma^+$ and form stable minima for WCO. In contrast, the ${}^7\Sigma^+$ state of MoCO does not form a minimum at all levels of theory, although the quintet states have minima in the potential surfaces and are above $Mo({}^7S) + CO({}^1\Sigma^+)$. Relativistic effects are found to stabilize WCO in contrast to MoCO. The lowest spin-orbit states arising from $W({}^5D)$ and $W({}^7S)$ are reversed in energy when spin-orbit effects were included consistent with the experimental atomic energy separations. The 0^+ state of WCO was found to undergo an avoided crossing due to spin-orbit coupling. The nature of bonding is discussed using the wave function composition and the Mulliken population analysis.

1. Introduction

Organometallic complexes of molybdenum and tungsten have been the topic of many recent experimental studies. Investigation of such complexes and their properties could aid not only in our comprehension of catalysis and chemisorption but also in the area of organic chemistry and biochemistry, because those complexes play an important role in these areas, too.^{1–6} The Mo-CO system has been employed as an oxidation and sulfidation agent and has thus attracted great attention.^{7,8} Synthesis, structure, and properties of these complexes have been the topic of several studies.^{9–13} Tungsten carbonyl species such as $W(CO)_2$ have been characterized by using the ultraviolet photoreduction method.¹⁴ The ground state of $W(CO)_n^+$ ($n = 1–6$) species have been studied theoretically at the ab initio level.¹⁵ Tungsten clusters such as W_3 clusters have been considered in our laboratory.¹⁶

In addition to the above applications, the study of the potential energy surfaces of MoCO and WCO could aid in our comprehension of atop chemisorption of CO on W and Mo surfaces. Typically in such atop chemisorption, a single metal atom is directly involved in the interaction of CO, and thus as demonstrated by our previous studies the computed properties of MCO ($M = \text{metal}$) exhibit remarkable resemblance to the experimentally measured properties such as CO stretching frequency in the atop mode of chemisorption on surfaces.

Relativistic effects could be important, especially for the tungsten-containing species.¹⁷ We expect not only mass-velocity contraction of the 6s orbital of the W atom to play an important role but also the large spin-orbit (SO) splitting of the 5d shell of the W atom to make a substantial impact into the properties of the electronic states of WCO. In particular, the electronic states would not get split by SO coupling but

different electronic states which do not normally mix in the absence of SO coupling could get coupled. This would also suggest a strong coupling between relativistic effects and electron correlation effects that make the third row transition-metal-containing species one of the most challenging sets of molecules for theoretical computations.

In the current study, we employ a complete active space multiconfiguration self-consistent field (CAS-MCSCF) technique to determine the potential curves and their corresponding electronic configurations. Higher order multireference singles + doubles configuration interaction (MRSDCI) computations were used to determine the minimum energies, the equilibrium bond-lengths, as well as the dissociation energies for the low-lying states. In addition, relativistic configuration interaction (RCI) calculations were also carried out to compute the potential energy curves with SO coupling and to assess the importance of the SO coupling effects. Mulliken populations and vibrational frequencies were computed from the wave functions.

2. Method of Calculations

Relativistic effective core potentials (RECPs) for both molybdenum and tungsten atoms were taken from Ross et al.¹⁸ which retained the outer $4s^2 4p^6 4d^5 5s^1$ and $5s^2 5p^6 5d^4 6s^2$ shells in the valence space, respectively. Likewise for the carbon and oxygen atoms, the RECPs retained the outer $2s^2 2p^2$ and $2s^2 2p^4$ shells in the valence space, respectively. The optimized (5s5p4d) valence Gaussian basis sets for the Mo and W atoms were taken from ref 18. The (4s4p) optimized Gaussian basis sets for the carbon and oxygen atoms were contracted to (3s3p). The carbon and oxygen basis sets were supplemented with a set of 3d functions generated from Dunning and Hay,¹⁹ with exponents $a_d = 0.75$ for carbon and $a_d = 0.85$ for oxygen, respectively. We have investigated the effect of 4f Gaussian functions on the metal atom in the past and found that these functions make very small contributions, especially at the

[†] Arizona State University.

[‡] Tsinghua University.

TABLE 1: Reference Configurations for the RCI Calculations of W–CO Including Spin–Orbit Interactions

configurations					λ -s state	ω - ω states				
1σ	2σ	3σ	1π	1δ		0^+	0^-	1	2	3
2	1	1	2	2	$7\Sigma^+$		56	35	54	49
2	1	1	3	1	5Φ			32	32	28
2	2	0	2	2	$5\Sigma^+$	18		12	17	
2	2	0	3	1	3Π	8	8	8	8	
2	1	0	4	1	3Δ			2	4	2
2	2	0	4	0	$1\Sigma^+$	1				
2	0	0	4	2	$1\Sigma^+$	4				
total reference configurations						31	64	89	115	79
total determinants						5077	8560	9848	12 762	10 004

MRSDCI level. The bond lengths change up to 0.01 Å, and energy separations change to a maximum of 0.01–0.1 eV. It should also be emphasized that relativistic effects including SO coupling (~ 5000 cm $^{-1}$) are far more important than the negligible effect of 4f-type of function. Consequently, in the present study more important relativistic effects are included and 4f functions are not included in the basis set.

The MoCO and WCO species were computed in the C_{2v} point group with the z axis chosen as the C_2 axis. According to the low-lying spectral terms of the Mo and W atoms,²⁰ we carried out in detail CASMCSCF calculations with one root for each electronic state of all possible spin multiplicities with different bond lengths varying from 1.4 to 8.0 Å. Let n_i represent the number of inactive orbitals and n_a the active orbitals in four irreducible representations in the C_{2v} group. At infinite separation between all atoms, the $(n-1)s$, $(n-1)p$, $(n-1)d$, and ns orbitals of Mo ($n=5$) or W ($n=6$), and $2s$, $2p$ orbitals of the carbon and oxygen atoms span 10 a_1 , four b_1 , four b_2 , and one a_2 under the C_{2v} symmetry. Among these, the semicore $(n-1)s$ and $(n-1)p$ orbitals of Mo or W, and the $2s$ and $2p$ orbitals of oxygen were found to be unimportant for the Mo + CO and W + CO interactions in the active space. These inactive orbitals thus comprise four a_1 , two b_1 , and two b_2 group orbitals. Excitations of electrons from the inactive orbitals were not allowed, but these orbitals were allowed to relax. The CASMCSCF computations thus included excitations of eight electrons in all possible ways among six a_1 , two b_1 , two b_2 , and one a_2 orbitals in active space. This choice, namely $n_i = 4,2,2,0$ (a_1, b_2, b_1, a_2) and $n_a = 6,2,2,1$, yields correct dissociation limit for both Mo + CO and W + CO.

The MRSDCI computations were carried out for the low-lying states, in which single and double excitations were allowed. Reference configurations were chosen from the CASMCSCF calculations. Configurations with coefficients ≥ 0.05 were chosen for the calculations. The CASMCSCF calculation included up to 12 740 configuration spin functions (CSFs), and the MRSDCI included up to 521 620 CSFs.

The SO effects were introduced through the RCI scheme developed by one of the authors.²¹ In this scheme all of the low-lying λ -s states which give rise to the same Ω quantum number were mixed in a multireference singles and doubles CI scheme including SO coupling. Table 1 shows a list of reference configurations included in the RCI for the various Ω states considered in this study. Consider the $\Omega = 2$ state as an example: this state contained 54 reference configurations from $1\sigma^2 2\sigma^1 3\sigma^1 1\pi^2 1\delta^2$ ($7\Sigma^+$), 32 reference configurations from $1\sigma^2 2\sigma^1 3\sigma^1 1\pi^3 1\delta^1$ (5Φ), 17 reference configurations from $1\sigma^2 2\sigma^2 1\pi^2 1\delta^2$ ($5\Sigma^+$), 8 reference configurations from $1\sigma^2 2\sigma^2 1\pi^3 1\delta^1$ (3Π), and 4 reference configurations from $1\sigma^2 2\sigma^1 1\pi^4 1\delta^1$ (3Δ). We have chosen 7 a_1 orbitals, 3 b_2 orbitals, 3 b_1 orbitals, and 2 a_2 orbitals as the active space for the spin-orbit computations. Single and double excitations from these

TABLE 2: Atomic Energy Separations of W + CO Obtained from Asymptotic Molecular Energy Separations at the Dissociation Limit^a

molecular state	dissociation limit	CASMCSCF (cm $^{-1}$)	MRSDCI (cm $^{-1}$)	expt. (cm $^{-1}$)
$7\Sigma^+$	(5d 5 6s) a 7 S + $1\Sigma^+$	0	0	0
$5\Sigma^+, 5\Pi, 5\Delta$	(5d 4 6s 2) a 5 D + $1\Sigma^+$	5342	1516	1506
$3\Pi, 3\Delta$	(5d 4 6s 2) a 3 P + $1\Sigma^+$	19 689	13 895	13 240
$7\Pi, 7\Delta$	(5d 4 6s6p) z 7 F + $1\Sigma^+$	22 751	21 524	22 556
$1\Sigma^+, 1\Pi, 1\Delta$	(5d 4 6s 2) a 1 G + $1\Sigma^+$	23 205	18 192	–

^a The distance between W and C is 8.00 Å.

reference configurations generated up to 12 762 determinants. The SO integrals derived from RECPs using Pitzer's Argos codes²² were transformed in the MRSDCI natural orbitals obtained in the absence of SO coupling. These integrals were then added to the CI Hamiltonian matrix in the RCI. All CASMCSCF/CI calculations were carried out by using one of the author's modified version of ALCHEMY II codes²³ to include RECPs.²⁴

3. Results and Discussion

A. Atomic Energy Separations of Mo and W. Tables 2 and 3 show a few possible molecular electronic states of W–CO and Mo–CO, respectively, derived from the atomic states. We set the distance between the metal atom and CO to 8.00 Å to obtain the energy separations at the dissociation limit. As seen from Tables 2 and 3, our computed atomic energy separations have been found to be in excellent agreement with the experimental values from Moore's atomic tables.²⁰ As expected, the MRSDCI calculations are in much better agreement with the experiment, because they included higher order correlation effects. The ground state of W is computed as a 7 S state arising from the 5d 4 6s 2 . The ground state of Mo is computed as a 7 S state arising from the 4d 5 5s 1 . We have obtained an averaged dissociation limit for the triplet state of the Mo complex because the 3P , 3D , 3F , and 3H spectral items of the molybdenum atom are quite close to each other, as seen from ref 20. The gross population of molybdenum for the triplet states at the dissociation limit is 4d 4 .⁴⁸5s 3 .⁴⁷ This is conceivably a combination of those atomic terms such as 3D from 4d 5 5s and 3P from 4d 4 6s 2 . The energy separation is computed as 29 864 and 26 133 cm $^{-1}$ above from ground state at the CASMCSCF and MRSDCI levels, respectively. Our computed R_e and ω_e values of the free diatomic CO obtained from the MRSDCI are 1.130 Å and 2202 cm $^{-1}$ compared to experimental values of 1.128 Å and 2170 cm $^{-1}$, respectively, in ref 25.

The SO effects are especially important for the W atom. The asymptotic energy separations of the electronic states including SO coupling were also computed to gauge the accuracy of SO effects for W. We shall discuss the actual results subsequently in the context of discussion of the SO effects (Section C).

TABLE 3: Atomic Energy Separations of Mo + CO Obtained from Asymptotic Molecular Energy Separations at the Dissociation Limit^a

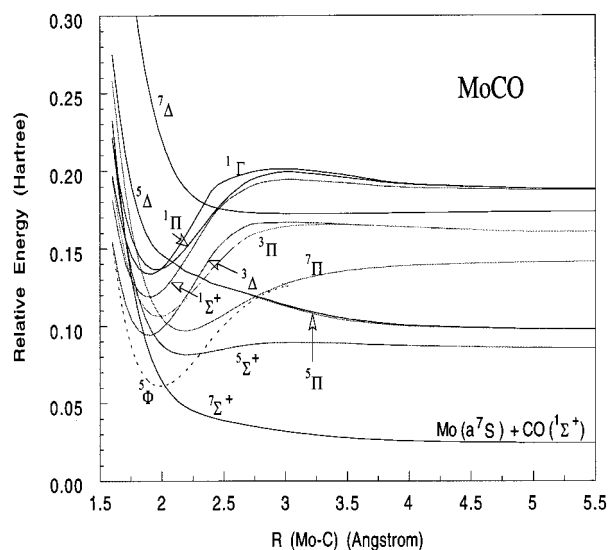
molecular state	dissociation limit	CASMCSF (cm ⁻¹)	MRSDCI (cm ⁻¹)	expt. (cm ⁻¹) ^a
$7\Sigma^+$	$(4d^5s) a^7S + ^1\Sigma^+$	0	0	0
$5\Sigma^+$	$(4d^5s) a^5S + ^1\Sigma^+$	13 414	11 847 (11 000)	10 768
$5\Pi, ^5\Delta$	$(4d^4s^2) a^5D + ^1\Sigma^+$	16 109	11 814 (10 989)	11 832
$3\Pi, ^3\Delta$	$[(4d^4s^2) a^3P - (4d^4s^2) a^3H] + ^1\Sigma^+$	29 864	26 133 (23 912)	21 258–24 506 ^b
7Π	$(4d^5p) z^7P + ^1\Sigma^+$	25 703	23 418 (23 049)	26 003
7Δ	$(4d^5s^2) z^7F + ^1\Sigma^+$	28 404	27 026 (26 710)	29 480
$1\Sigma^+, ^1\Pi, ^1\Delta$	$(4d^4s^2) a^1G + ^1\Sigma^+$	35 842	30 235 (28 356)	26 636

^a The distance between Mo and C is 8.00 Å. ^{b,c} Relative energy at the dissociation limit from $(4d^4s^2)a^3P$ to $(4d^4s^2)a^3H$.

TABLE 4: The Spectroscopic Properties and Energy Separations of Electronic States of MoCO^a

state	CASMCSF						MRSDCI					
	Mo–C (Å)	C–O (Å)	Mo–O (Å)	T_e (cm ⁻¹)	ω_e (cm ⁻¹)	D_e (eV)	Mo–C (Å)	C–O (Å)	T_e (cm ⁻¹)	ω_e (cm ⁻¹)	D_e (eV)	
$7\Sigma^+$						0					0	
$5\Sigma^+$	2.213	1.114	3.327	0	2183	-1.51	2.154	1.113	0 (0)	2183	-0.851	
5Φ	1.992	1.154	3.146	-4280	2190	-0.982	1.994	1.153	3305 (4483)	2196	-1.26	
3Δ	1.900	1.161	3.061	2838	2204	-1.86	1.894	1.160	3643 (3413)	2202	-1.30	
7Π	2.191	1.127	3.318	3625	2034	-1.96	2.161	1.132	4192 (5276)	2069	-1.37	
3Π	1.981	1.146	3.127	5710	2167	-2.22	1.975	1.144	5540 (4166)	2163	-1.54	

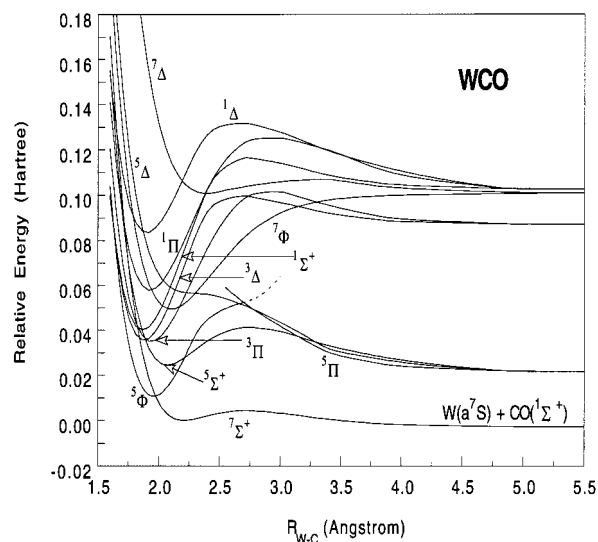
^a ω_e stands for the vibrational frequency of the C–O bond. The values in parentheses are the Davidson corrected energies.

**Figure 1.** Potential energy curves for Mo–CO.

B. Potential Energy Curves of Mo–CO and W–CO.

Figures 1 and 2 show the CASMCSF potential energy curves of the low-lying states of Mo–CO and W–CO, respectively. As discussed in ref 26, the M–OC complex, where M stands for a transition metal, is found to be considerably higher in energy compared to M–CO. In the current study, we thus investigate only Mo–CO and W–CO complexes. As seen from Figure 1, $7\Sigma^+$ was found to be the lowest for Mo–CO but it is repulsive, in contrast to WCO (Figure 2) which forms a minimum.

Table 4 shows the actual equilibrium geometries, spectroscopic properties, and the relative energy separations of the bound electronic states of Mo–CO at both CASMCSF and MRSDCI levels. As seen from Table 4 as well as Figure 1, the lowest state of MoCO is $7\Sigma^+$, but it was found to be an unstable state. However, the quintet states, namely 5Φ and $5\Sigma^+$, were found to have minimum in their potential energy surfaces, although these are above the $Mo(^7S) + CO(^1\Sigma^+)$ dissociation limit. We have calculated the equilibrium distances of 5Φ as $R_e(\text{Mo–C}) = 1.992$ and $R_e(\text{C–O}) = 1.154$ Å at the CASMCSF level, and these values become 1.994 and 1.153 Å at the MRSDCI level. For $5\Sigma^+$, the equilibrium geometry was found

**Figure 2.** Potential energy curves for W–CO.

to be $R_e(\text{Mo–C}) = 2.213$ and $R_e(\text{C–O}) = 1.114$ Å at the CASMCSF level, and the corresponding values are 2.154 and 1.113 Å at the MRSDCI level. Most of the electronic states are above the $Mo(a^7S) + CO(^1\Sigma^+)$ dissociation limit. The relative order of electronic states changes as the level of theory changes. We have also calculated the bond length and frequency of the C–O bond for the low-lying states of MoCO, as shown in Table 4. High order correlation effects included in the MRSDCI generally shrink the metal–carbon bond. As expected, the R_e of Mo–C of the $5\Sigma^+$ state shrinks by 0.06 Å at the MRSDCI level compared to the CASMCSF results, and the R_e of 5Φ by shrinks 0.002 Å. On the other hand, the equilibrium C–O bond distances and the CO vibrational frequencies do not change too much, as seen from Table 4. Our computed CO vibrational frequency values for most of the states are around 2050–2220 cm⁻¹, suggesting about 7% reduction in the CO vibrational frequency in MoCO with respect to the free CO frequency of 2260 cm⁻¹ at the MRSDCI level.

Table 5 shows the equilibrium geometries, spectroscopic properties, and the energy separations of the low-lying electronic states of W–CO at both CASMCSF and MRSDCI levels. As seen from this table as well as Figure 2, although the $7\Sigma^+$, 5Φ ,

TABLE 5: The Spectroscopic Properties and Energy Separations of Electronic States of WCO without Spin–Orbit Effect^a

state	CASMCSCF						MRSDCI				
	W–C (Å)	C–O (Å)	W–O (Å)	T_e (cm ⁻¹)	ω_e (cm ⁻¹)	D_e (eV)	W–C (Å)	C–O (Å)	T_e (cm ⁻¹)	ω_e (cm ⁻¹)	D_e (eV)
${}^7\Sigma^+$	2.221	1.122	3.343	0	2176	-0.053	2.195	1.123	0 (0)	2176	0.276
${}^5\Phi$	1.965	1.158	3.123	2335	2210	-0.342	1.960	1.157	266 (-37)	2202	0.244
${}^5\Sigma^+$	2.084	1.123	3.207	5375	2172	-0.719	2.075	1.122	720 (-742)	2177	0.187
${}^3\Delta$	1.887	1.167	3.054	7574	2212	-0.992	1.887	1.166	5092 (3990)	2204	-0.355
${}^3\Pi$	1.944	1.150	3.094	7774	2195	-1.017	1.940	1.148	2991 (1108)	2192	-0.162
${}^1\Sigma^+$	1.875	1.162	3.037	8698	2208	-1.131	1.867	1.159	4321 (2833)	2202	-0.259

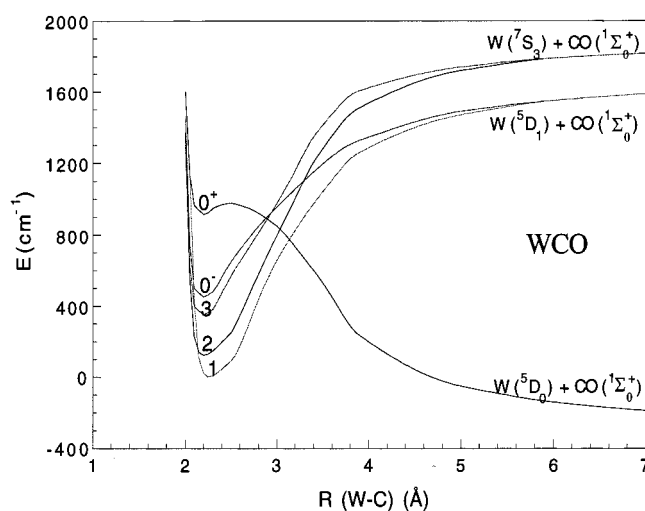
^a ω_e stands for the vibrational frequency of the C–O bond. The values in parentheses are the Davidson corrected energies.

TABLE 6: Spectroscopic Constants of the Low-Lying States of W–CO Including Spin–Orbit Effects

$\omega-\omega$ state	main components (%)					W–C, Å		C–O, Å		T_e , cm ⁻¹		ω_e , cm ⁻¹	
	${}^7\Sigma^+$	${}^5\Sigma^+$	${}^3\Delta$	${}^3\Pi$	${}^3\Sigma^-$	SO	NO SO	SO	NO SO	SO	NO SO	SO	NO SO
3	96.8		0.1			2.188	2.195	1.123	1.123	-417	0	2175	2176
2	96.9	1.8	1.0			2.167	2.195	1.124	1.123	-645	0	2172	2176
1	91.7					2.187	2.195	1.123	1.123	-768	0	2176	2176
0 ⁻	95.7					2.191	2.195	1.122	1.123	-318	0	2262	2176
0 ⁺		78		6.5	7	2.073	2.075	1.122	1.122	149	720	2196	2177

and ${}^5\Sigma^+$ states are almost degenerate for WCO, quintet states are favored as more electron correlation effects are included. The equilibrium distances are $R_e(\text{W–C}) = 2.221$ and $R_e(\text{C–O}) = 1.122$ Å at the CASMCSCF level for ${}^7\Sigma^+$, and they become 2.195 and 1.123 Å at the MRSDCI level. We have also calculated the equilibrium distance and vibrational frequency of the C–O bond for the low-lying states, as seen from Table 5. The MRSDCI calculations shrink the W–C bond distance of the ${}^7\Sigma^+$ state by 0.02 Å compared to the CASMCSCF results. The equilibrium distance of the C–O bond remains about the same. Our computed CO vibrational frequency values for most of the states of WCO are between 2150 and 2210 cm⁻¹, suggesting a 5% reduction of the CO stretching frequency in WCO with respect to the free CO frequency of 2260 cm⁻¹ at the MRSDCI level. The dissociation energies (D_e) of the ${}^7\Sigma^+$ ground state of W–CO with respect to the $\text{W}(\text{a}^7\text{S}) + \text{CO}({}^1\Sigma^+)$ dissociation limit are computed as -0.053, 0.242, and 0.339 eV at the CASMCSCF, MRSDCI, and MRSDCI + Q levels, respectively. Quintet states, such as ${}^5\Phi$ and ${}^5\Sigma^+$, have higher D_e values (0.344 and 0.431 eV, respectively) than the ${}^7\Sigma^+$ state as more electron correlation effects are included. A recent study¹⁵ has considered the ground states of cations of tungsten carbonyl complexes such as $\text{W}(\text{CO})_n^+$ ($n = 1-6$) at the ab initio level without inclusion of spin–orbit coupling. For WCO^+ , ${}^6\Sigma^+$ was found to be the ground state, and ${}^4\Phi$ was the first excited state. These states are obtainable by ionizing an electron from ${}^7\Sigma^+$ or ${}^5\Phi$, as obtained from our result. The D_e values of ${}^6\Sigma^+$ and ${}^4\Phi$ were found to be 2.33 and 1.49 eV, respectively. Thus the positive ions of the complex are considerably more stable.

C. SO Effects for W–CO. Figure 3 shows our computed potential energy curves of the electronic states of WCO including SO effects. These curves were obtained by applying the SO corrections derived from the RCI on the MRSDCI energies which do not include SO correction. Table 6 shows the effect of SO coupling on the low-lying electronic states of W–CO near their equilibrium distances. The SO states are designated by their Ω numbers. Two nearly degenerate electronic states were found as candidates for the ground state of WCO when SO effects were included ($\Omega = 1$ and 2 states), but other electronic states such as $\Omega = 3, 1, 0^-$ states are quite close to $\Omega = 1$ and 2. The biggest SO effect on the equilibrium distance of the W–C bond is found for the $\Omega = 2$ state, with $W\text{–C} = 2.167$ Å when SO coupling is included, compared with $W\text{–C} = 2.195$ Å without SO correction. The SO coupling has

**Figure 3.** The potential energy curves for W–CO including spin–orbit effects, obtained by spin–orbit corrections to MRSDCI energies.

only a small effect on the equilibrium bond distance and the vibrational frequency of C–O as expected. The states with $\Omega = 3, 2, 1, 0^-$ are dominated by ${}^7\Sigma^+$, and the state with $\Omega = 0^+$ is dominated by ${}^5\Sigma^+$. This suggests that the structures of the electronic states of the W–CO complex are changed very little when the SO effect has been included, but the T_e values are influenced to a greater extent by the SO correction. The ${}^7\Sigma^+$ ground state does not mix with other low-lying states as much when SO coupling is included.

As seen from Figure 3, the SO coupling has an interesting effect on the electronic states as a function of the W–C distance. Most interesting is the 0^+ electronic state, which is higher than the manifold of 1, 2, 3, and 0^- SO states near the minimum, but at longer distances the 0^+ state becomes substantially lower leading to the $\text{W}({}^5\text{D}_0) + \text{CO}$ dissociation limit which falls below the $\text{W}({}^7\text{S}_3) + \text{CO}$ dissociation limit. This is indeed interesting and noteworthy in that in the absence of SO coupling the $\text{W}({}^7\text{S}) + \text{CO}$ dissociation limit (see Figures 1 and 2) is lower than the $\text{W}({}^5\text{D}) + \text{CO}$ dissociation limit.

Table 7 compares our computed SO energy separations of the W atom compared to the experimental energy level separations of the W atom as found in Moore's²⁰ atomic tables. Our computations reproduce the $\text{W}({}^5\text{D}_0)\text{–}\text{W}({}^5\text{D}_1)$ energy separation quite well compared to the experiment. It is also

TABLE 7: Atomic Energy Separations of W–CO at the Dissociation Limit Including Spin–Orbit Effects^a

$\omega-\omega$ state	W + CO	ΔE , theory (cm ⁻¹)	ΔE , expt. (cm ⁻¹)
0 ⁺	(⁵ D ₀) + ¹ Σ ₀ ⁺	0	0
1, 0 ⁻	(³ D ₁) + ¹ Σ ₀ ⁺	1776	1670
3,2,1,0 ⁻	(⁷ S ₃) + ¹ Σ ₀ ⁺	2004	2951

^a The distance between W and C is 8.00 Å.

TABLE 8: Leading Configurations in the MRSDCI Wave Function of the Low-Lying Electronic States of W–CO and Mo–CO

state	weights (%)		configurations					
	MoCO	WCO	2σ	3σ	4σ	1π	2π	1δ
⁷ Σ ⁺	97	94	1	1	0	2	0	2
⁵ Σ ⁺	71	78	2	0	0	2	0	2
	7	5	1	1	0	2	0	2
⁵ Φ	87	90	1	1	0	3	0	1
³ Δ	85	86	1	0	0	4	0	1
⁷ Φ		98	1	1	0	2	1	1
⁷ Π	94		1	0	0	2	1	2
³ Π	40	76	2	0	0	3	0	1
	35	4	1	0	0	3	0	2
¹ Π	57	76	2	0	0	3	0	1
	19	14	1	0	0	3	0	2
¹ Σ ⁺	30	74	2	0	0	4	0	0
	58	4	0	0	0	4	0	2
¹ Γ	90		0	0	0	4	0	2
¹ Δ		88	1	0	0	4	0	1
⁵ Δ	86		1	1	0	2	0	2
	3	70	2	1	0	2	0	1
		10	1	0	0	2	0	3
⁷ Δ	98	98	1	1	1	1	1	1

noteworthy that the W(⁷S₃) state which arises from a different manifold (5d⁵6s¹) is computed reasonably well.

The analysis of the RCI weights of the various electronic states of WCO including SO coupling reveals an interesting trend. As seen from Table 6, near the minima the 3, 2, 1 and 0⁻ electronic states are predominantly composed of the ⁷Σ⁺ state. On the other hand, the 0⁺ electronic state exhibits an avoided crossing due to SO coupling. At 1.70 Å the 0⁺ state is 59% ³Π, 21% ¹Σ⁺, and 7% ³Σ⁻, and at 2.1 Å it becomes 78% ⁵Σ⁺, 7% ³Π, and 7% ³Σ⁻. This is consistent with the curves in Figure 2 which suggest the possibility of substantial interaction among these states. At shorter distances the contribution of ³Π increases, which is consistent with Figure 2, and at the dissociation limit a different behavior is observed for this state. At 8.0 Å the 0⁺ state becomes 88% ⁵Σ⁺, 0.3% ³Π, and 4% ³Σ⁻ which is consistent with a pure W(⁵D₀) + CO dissociation, where the W state arises from 5d⁴6s².

D. The Nature of the Low-Lying Electronic States of Mo–CO and W–CO. Table 8 shows the leading configurations in the MRSDCI wave functions of the low-lying electronic states for Mo–CO and W–CO without SO interaction. The

⁷Σ⁺ ground state (lowest repulsive state of Mo–CO) is predominantly composed of 1σ²2σ¹3σ¹1π²1δ² with a coefficient ≥ 0.94. The ⁵Σ⁺ state is formed from the ⁷Σ⁺ state by moving the 3σ electron to 2σ to generate a doubly occupied 2σ orbital. The ⁵Φ state is generated by exciting an electron from the 1δ orbital to the 1π orbital, which lowers the spin multiplicity.

The Mulliken populations of the low-lying states of Mo–CO and W–CO are presented in Table 9. The standard description of bonding of metal carbonyls is one of donation from the highest occupied σ orbital (which is essentially a carbon lone pair) to the metal atom followed by a π back-donation from the metal atom to the carbonyl π* antibonding orbital with a large carbon component. We have also presented the population analysis at the dissociation limit for the ⁷Σ⁺ state. As seen from Table 9, ⁷Σ⁺ at the dissociation limit is composed of Mo(s^{3.001}p^{6.009}d^{5.010}), C(2s^{1.749}2p^{1.829}), and O(2s^{1.820}2p^{4.469}), which indicates that the Mo population is near its atomic level; the carbon and oxygen atoms remain in the diatomic CO together. The ⁵Σ⁺ state is composed of Mo(s^{2.873}p^{6.115}d^{4.868}), C(2s^{1.507}2p^{2.130}), and O(2s^{1.923}2p^{4.449}). The free Mo and CO populations obtained from the Mo(a⁵S) + CO(1Σ⁺) dissociation limit are Mo(s^{2.971}p^{6.058}d^{4.982}), C(2s^{1.752}2p^{1.827}), and O(2s^{1.820}2p^{4.468}). Thus, in the Mo–CO bond formation, there is a primary transfer of electron density from the carbon 2s orbital (0.25e) to the molybdenum. Molybdenum in turn loses 0.1e from its 5s orbital and donates about 0.11e charge from its dπ orbital to the π* orbital of CO. Consequently, the gross populations of molybdenum, carbon, and oxygen are only slightly changed compared to the populations at the dissociation limit.

Relativistic mass–velocity effect¹⁷ is primarily responsible for the contraction and stabilization of the 6s orbital of the W atom, and thus the 6s orbital of W can more readily accept the electric charge from the carbon atom followed by back-donation of electronic charge from W to the π* antibonding orbital of CO. The ⁷Σ⁺ ground state of W–CO is composed of W(s^{3.124}p^{6.176}d^{4.440}), C(2s^{1.539}2p^{2.130}), and O(2s^{1.959}2p^{4.496}). The free W and CO populations obtained from the W(a⁷S) + CO(1Σ⁺) dissociation limit are W(s^{2.999}p^{6.022}d^{4.980}), C(2s^{1.749}2p^{1.830}), and O(2s^{1.820}2p^{4.469}). Thus, in the W–CO bond formation, there is primary transfer of electron density from the carbon 2s orbital (0.21e) to the tungsten. Tungsten in turn donates about 0.54e charge from the dπ orbital to the pπ orbital of CO. Consequently, the tungsten 6s orbital gains 0.21e from carbon. The net population of tungsten and carbon atoms decreases by about 0.26 and 0.24e, respectively, while enhancing 0.5e on oxygen. This feature of Mulliken population suggests that the electron transfer from CO originates from the lone pair on carbon resulting in a σ bond, and the electronic charge transfer from the metal leads to dπ–pπ back-bonding. The populations of the s and p orbitals for oxygen are about the same, but for carbon

TABLE 9: Mulliken Population Analysis for the Low-Lying Electronic States of MoCO and WCO

species	state	gross population									
		O	C	M	O (s)	O (p)	C (s)	C (p)	M (s)	M (p)	M (d)
MoCO	⁷ Σ ⁺ ^a	6.334	3.666	14.00	1.820	4.469	1.749	1.829	3.001	6.009	5.010
	⁵ Σ ⁺	6.420	3.725	13.86	1.923	4.449	1.507	2.130	2.873	6.115	4.868
	⁵ Φ	6.506	3.860	13.63	1.909	4.553	1.439	2.330	2.583	6.009	5.043
	³ Δ	6.544	3.757	13.70	1.907	4.593	1.354	2.295	2.925	6.016	4.758
WCO	⁷ Σ ⁺	6.501	3.759	13.74	1.959	4.496	1.539	2.130	3.124	6.176	4.440
	⁵ Σ ⁺	6.478	3.685	13.84	1.952	4.479	1.406	2.190	3.406	6.165	4.266
	⁵ Φ	6.565	3.904	13.53	1.948	4.573	1.426	2.379	2.729	6.062	4.740
	³ Π	6.538	3.818	13.64	1.946	4.548	1.389	2.328	3.034	6.135	4.475

^a This repulsive state was analyzed at the dissociation limit.

and tungsten there has been a great change according to the states. For example, the gross populations of the $^5\Sigma^+$ and $^5\Phi$ states are $W(s^{3.406}p^{6.165}d^{4.266})$, $C(2s^{1.406}2p^{2.190})$, and $W(s^{2.729}p^{6.062}d^{4.740})$, and $C(2s^{1.426}2p^{2.379})$, respectively.

4. Conclusion

We obtained the potential energy curves and spectroscopic properties of the low-lying states of Mo–CO and W–CO arising from several dissociation limits including $M(a^7S) + CO(^1\Sigma^+)$ ($M = Mo, W$). Three nearly-degenerate electronic states ($^7\Sigma^+$, $^5\Phi$, and $^5\Sigma^+$) were found as candidates for the ground state of WCO. The $^7\Sigma^+$ state is not bound for MoCO, but quintet states were found to be bound. The ground state of W–CO including SO effects was found to be a $\Omega = 2$ state. Other states, such as $\Omega = 3, 1, 0^-$ are quite close to the $\Omega = 2$ state. The spin-orbit effects on energy separations are more significant compared to the geometries. The nature of the low-lying electronic states is discussed through the CI coefficients and the Mulliken populations.

Acknowledgment. This research was supported by the U.S. Department of Energy under Grant No. DEFG02-86ER13558.

References and Notes

- (1) Chernega, A. N.; Graham, A. J.; Souter, J. *J. Chem. Soc., Dalton Trans.* **1997**, 2293.
- (2) Young, C. G.; Wedd, A. G. *Chem. Commun.* **1997**, 14, 1251.
- (3) Collison, D.; Garner, C. D.; Joule, J. A. *Chem. Soc. Rev.* **1996**, 25, 25.
- (4) Gruselle, M.; Kondratenko, M. A.; Rager, M. N. *Organometallics* **1995**, 14, 3802.
- (5) Barrado, G.; Li, J.; Miguel, D. *Organometallics* **1994**, 13, 2330.
- (6) LaBrie, S. T.; Crawford, N. M. *J. Biol. Chem.* **1994**, 269, 14497.
- (7) Spencer, N. D.; Pereira, C. J. *J. Catal.* **1989**, 116, 399.
- (8) Ramselaar, W. L. T. M.; Craje, M. W. J.; Gerkema, E. *Appl. Catal.* **1989**, 54, 217.
- (9) Chisholm, M. H.; Huang, J. H.; Parkin, I. P. *Inorg. Chem.* **1997**, 36, 1642.
- (10) Hill, A. F.; Malget, J. M. *J. Chem. Soc., Dalton Trans.* **1997**, 12, 2003.
- (11) Novoselova, I. A.; Malyshev, V. V.; Shapoval, V. I. *Russ. J. Inorg. Chem.* **1995**, 40, 1384.
- (12) Woodworth, B. E.; Templeton, J. L. *J. Am. Chem. Soc.* **1996**, 118, 7418.
- (13) Slugovc, C.; Mauthner, K.; Kirchner, K. *Organometallics* **1996**, 15, 2954.
- (14) Kohler, S.; Kohler, S. D.; Ekerdt, J. G. *J. Phys. Chem.* **1994**, 98, 1276.
- (15) Buker, H. H.; Maitre, P.; Ohanessian, G. *J. Chem. Phys.* **1997**, 101, 3966.
- (16) Balasubramanian, K.; Dai, D. *Chem. Phys. Lett.* **1997**, 265, 538.
- (17) Balasubramanian, K. *Relativistic Effects in Chemistry. Part A: Theory and Techniques*; Wiley-Interscience, New York, 1997; p 301; *Relativistic Effects in Chemistry. Part B: Applications*; Wiley-Interscience: New York, 1997; p 531.
- (18) Ross, R. B.; Powers, J. M.; Atashroo, T.; Ermler, W. C. *J. Chem. Phys.* **1990**, 93, 6654.
- (19) Dunning, T. H., Jr.; Hay, P. J. In *Methods of Electronic Structure Theory*; Schaefer III, H. F., Ed.; Plenum: New York, 1977; p 1.
- (20) Moore, C. E. *Tables of Atomic Energy Levels*; National Bureau of Standards: Washington, DC, 1971.
- (21) Balasubramanian, K. *J. Chem. Phys.* **1988**, 89, 5731.
- (22) Pitzer, R. M.; Winter, N. W. *J. Phys. Chem.* **1988**, 92, 3061.
- (23) The major authors of ALCHEMY II are Lengsfeld, B.; Liu, B.; Yoshimine, Y.
- (24) Balasubramanian, K. *Chem. Phys. Lett.* **1986**, 127, 585.
- (25) Huber, K. P.; Herzberg, G. *Molecular Spectra and Molecular Structure IV, Constants of Diatomic Molecules*; Van Nostrand Reinhold: New York, 1979.
- (26) Dai, D.; Balasubramanian, K. *J. Chem. Phys.* **1994**, 101, 2148.